

3D Layer-Integrated Modelling of Morphodynamic Processes Near River Regulated Structures

S. Faghihrad^{1,2} · B. Lin^{2,3} · R. A. Falconer²

Received: 12 December 2014 / Accepted: 30 October 2016 /

Published online: 23 November 2016

© The Author(s) 2016. This article is published with open access at Springerlink.com

Abstract Sedimentation and erosion can significantly affect the performance of river regulated reservoirs. In the vicinity of flow control structures, the interaction between the hydrodynamics and sediment transport often induces complex morphological processes. It is generally very challenging to accurately predict these morphological processes in real applications. Details are given of the refinement and application of a three-dimensional (3-D) layer integrated model to predict the morphological processes in a river regulated reservoir. The model employs an Alternating Direction Implicit finite difference algorithm to solve the mass, momentum and suspended sediment transport conservation equations, and an explicit finite difference scheme for the bed sediment mass conservation equation for calculating bed level changes. The model is verified against experimental data reported in the literature. It is then applied to a scaled physical model of a regulated reservoir, including the associated intakes and sluice gates, to predict the velocity distributions, sediment transport rates and bed level changes in the vicinity of the hydraulic structures. It is found that the velocity distribution near an intake is non-uniform, resulting in a reduction in the suspended sediment flux through the intake and the formation of a sedimentation zone inside the reservoir.

Keywords Morphodynamics · Numerical modelling · Turbulent flows · Regulated reservoirs · Three-dimensional flow · Physical modelling · Laboratory studies

✉ B. Lin
LinBL@tsinghua.edu.cn

¹ Water Research Institute, Tehran, Iran

² Hydro-Environmental Research Centre, School of Engineering, Cardiff University, Cardiff CF24 3AA, UK

³ Hydro-Science Key Laboratory, Tsinghua University, Beijing, China 100084

1 Introduction

In order to better understand the impact of hydraulic structures on the hydrodynamic, sediment transport and morphological processes in reservoirs and rivers, it is often necessary to use numerical and/or physical models to investigate these dynamic and interacting processes.

The three dimensionality of turbulence and the sediment transport and morphological processes in the vicinity of hydraulic structures form a complex problem. Khan et al. (2012) developed a reservoir simulation model with the genetic algorithm based optimization capabilities. Pu et al. (2013) compared different numerical modelling techniques for simulating water flows and transport processes. De Vriend (1985, 1986) studied the theoretical basis and the performance of two-dimensional (2-D) and three-dimensional (3-D) morphological models. van Rijn (1987) used a width-averaged two-dimensional numerical model to simulate bed level changes in a dredged trench. The numerical model predicted bed level changes agreed closely with the data measured from scaled physical model experiments. Martinez et al. (1999) used a 2-D depth-averaged finite element model to predict the evolution process of bed elevation, as well as the distribution of suspended sediment concentrations in a model harbour. Olsen (1999) applied a 2-D depth-averaged numerical model to calculate bed level changes in a reservoir which was flushed by flood flows. Kocyigit et al. (2005) presented the refinement of a 2-D depth-integrated numerical model for predicting the long-term bed level changes in an idealised model harbour. They reported an under-prediction of the depth of erosion, which was thought to be due to the model not correctly predicting the lateral movement of sediment.

Olsen (1999) undertook a 3-D numerical model study of bed level changes in a sand trap. The numerical model results compared well with the measurements obtained from a physical model study. Gessler et al. (1999) developed a 3-D model of river morphology, which included separate solvers for bed load transport and suspended sediment transport. The model included several size fractions of sediment and recorded the bed composition and evolution during each time step. Kolahdoozan and Falconer (2003) developed a three-dimensional layer-integrated morphological model for estuarine and coastal waters and compared the numerical model predictions with experimental measurements, obtained from a scaled laboratory model harbour. They used the mixing length model for turbulence closure, and recommended that a fine mesh should be used in areas of severe erosion or deposition. Olsen (2003) and R uther and Olsen (2003, 2005a, b) developed a fully three dimensional model with an unstructured grid and showed model predictions of the evolution of a meandering channel. Their work focused on the formation of alternate bars and the initiation of a meandering channel starting from a straight channel.

In many research projects physical and numerical models have been used jointly to better understand the hydrodynamic and sediment transport processes in free surface flows. Stephan and Hengel (2010) used a physical model to obtain improvements in understanding and predicting the sediment transport processes through the backwater of a hydropower plant. Wan et al. (2010) and investigated sediment deposition in a reservoir and Khan et al. (2012) using a sediment evacuation model to minimize irrigation deficits. The 3-D morphodynamic model SSIIM (Olsen 2003) was applied in this case in order to reproduce the erosion and deposition patterns. The numerical model results agreed well with the experimental erosion and deposition patterns, but there were some differences between the model predicted and measured bed levels.

In the current study a layer integrated three-dimensional model has been refined to predict the morphological processes in a river regulated reservoir. Sedimentation and erosion can

significantly affect the performance of river regulated reservoirs. The velocity distribution is usually complex near the control structures, which can induce complex sediment transport and morphological processes. It is generally very challenging to accurately predict these morphological processes for real applications. The main objective of this research study is to refine a three-dimensional morphodynamic model to predict more accurately the sedimentation processes and bed level changes in the vicinity of hydraulic structures. The original model was developed by Hakimzadeh and Falconer (2007) for simulating re-circulating flows in tidal basins. Improvements were made to the model in order to predict more accurately the hydrodynamic and sediment transport processes in river and reservoirs (Faghihirad et al. 2010). The model has been applied to investigate the hydrodynamic and suspended sediment transport processes in a river regulated reservoir (Faghihirad et al. 2015).

In the current study, a new module has been added to the code for predicting the morphodynamic processes. In order to be consistent with the sediment transport model, an explicit finite difference scheme was used to solve the sediment mass conservation equation to enable predictions of bed level changes. The model was tested against data observed from two laboratory experiments reported in the literature, and then it was applied to a scaled physical model of a regulated reservoir. Numerical model results were compared with measured laboratory data, with comparisons also being made against predictions obtained using some other numerical models.

2 Material and Methods

2.1 Project Background

The regulated reservoir studied in this project is located 11 km away from Hamidieh Town, along the Karkhe River, downstream of the Karkhe reservoir dam, in Iran. Currently there are two water intakes, named the Vosaikeh and Ghods intakes. The Vosaikeh water intake channel is 10.8 km long, with a maximum discharge of 60 m³/s, while Ghods intake operates through a 2.5 km long channel with a maximum discharge capacity of 13 m³/s.

Due to the development in irrigation and drainage networks in the Azadegan and Chamran regions, the existing intakes are no longer able to meet the water demand. Hence, it is necessary to increase the flow rates of these intakes by building new water intake structures.

The planned Hamidieh reservoir dam is 192 m long, 4.5 m high and with 19 spillway bays and 10 sluice gates. A new water intake for Azadegan, with an inlet width of 56 m, 8 opening bays and 4 under sluice gates, will be built to replace the Ghods water intake. The aim of the new scheme is to increase the discharge capacity from 13 m³/s to 75 m³/s. The Vosaikeh water intake will also be replaced by a new water intake for Chamran, with an inlet width of 86.6 m, 16 opening bays and 13 trash racks opening, to increase the discharge capacity from 60 m³/s to 90 m³/s. Figure 1 shows a plan view of the Hamidieh regulated reservoir and associated structures.

An undistorted 1/20-scale physical model of the reservoir and its relevant structures was constructed and experiments were undertaken by the first author to investigate the hydrodynamic, sediment transport and morphodynamic processes in the reservoir. The aim was to better understand the operation of the entire system and to improve the flow and sediment behaviour near the structures.

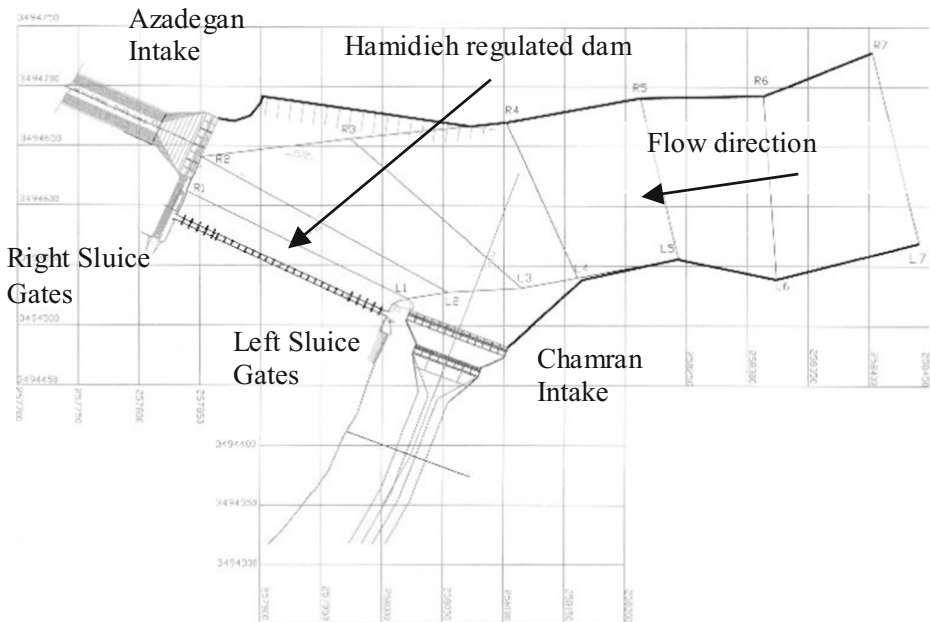


Fig. 1 Plan of Hamidieh regulated dam (Faghihirad et al. 2010)

This study is a part of an integrated research study to investigate the hydrodynamic, sediment transport and morphodynamic processes in the Hamidieh reservoir. The hydrodynamic and sediment transport studies were carried out before and full details of the numerical simulation procedure are given in Faghihirad et al. (2015) and are not included here for brevity.

The bathymetric data and morphodynamic scenarios were defined by using field surveyed and laboratory measured data. Table 1 lists the hydraulic and sediments parameters used to set-up the numerical model for testing the morphodynamic model scenarios. These parameters were chosen on the basis of the data obtained from the physical model experiments.

2.2 Numerical Model

The numerical model used to simulate the morphodynamic processes comprises three separate modules including: the hydrodynamic, sediment transport and bed-level change modules. The hydrodynamic governing equations are solved using a combined layer-integrated and depth-integrated scheme (Lin and Falconer 1997), with the two-equation $k-\varepsilon$ model being used for turbulence closure (Hakimzadeh and Falconer 2007). The operator splitting technique and a highly accurate finite difference scheme are used to solve the suspended sediment transport equation (Lin and Falconer 1996). A new solution of the depth-integrated mass balance equation has been developed to determine the bed level change due to sediment transport.

2.2.1 Layer Integrated Hydrodynamic Model

In the layer integrated numerical the governing mass and momentum equations were solved using the finite difference scheme on a regular square mesh in the horizontal plane, and a layer-integrated finite difference scheme on an irregular mesh in the vertical plane. A sketch of the

Table 1 Hydraulic and sediment parameters of morphodynamic scenarios

No		Operation	Boundary Condition	Concentration (gr/litre)	Time for simulation (hour)
S.1	Reservoir	Water level 1.0225 m	Discharge 70.9 l/s	0.2321	48.5
	Az Intake	Open	Discharge 41.9 l/s	–	
	Ch Intake	Open	Water level 1.0225 m	–	
	L S	Closed	–	–	
	R S	Closed	–	–	
S.2	Reservoir	Water level 1.0225 m	Discharge 95.3 l/s	0.679	8
	Az Intake	Open	Discharge 39.7 l/s	–	
	Ch Intake	Open	Water level 1.0225 m	–	
	L S	Open	Water level 1.0225 m	–	
	R S	Closed	–	–	
S.3	Reservoir	Water level 1.0225 m	Discharge 167.7 l/s	2.122	8
	Az Intake	Open	Discharge 39.7 l/s	–	
	Ch Intake	Open	Water level 1.0225 m	–	
	L S	Open	Water level 1.0225 m	–	
	R S	Open	Water level 1.0225 m	–	
General data d_{16}, d_{50}, d_{84} & $d_{90} = 0.0015, 0.0076, 0.0166$ & 0.0236mm <i>SepecificGravity</i> = 2.67, <i>Grid size</i> = 0.25 m					

Az Intake = Azadegan Intake, Ch Intake = Chamran Intake, L S = Left sluice gates and R S = Right sluice gates

3D grid and the relative positions of the governing variables in the $x-z$ plane are illustrated in Fig. 2. As illustrated, three layer types exist, including a top layer, bottom layer and middle layer. The top and bottom layer thicknesses vary with the x, y co-ordinates, to prescribe both the free surface and bottom topography, respectively. In contrast, the middle layers have a uniform (or non-uniform) thickness.

The eddy viscosity concept has been used to represent the Reynolds stresses. The horizontal eddy viscosity was assumed to be constant along the water depth, with the depth-averaged eddy viscosity value being set for all layers.

The depth-integrated horizontal eddy viscosity was calculated (after Fischer et al. 1979) using:

$$\varepsilon_h = \sigma \frac{H}{C} \sqrt{g(U^2 + V^2)} \quad (1)$$

where σ = eddy viscosity coefficient, C = Chezy roughness coefficient ($m^{1/2}/s$), H = depth of flow (m), U, V = depth average velocity components in the x and y directions (m/s), respectively.

The vertical eddy viscosity was evaluated using the layer integrated form of the $k-\varepsilon$ equations based on Hakimzadeh (1997). The two equations were discretised using a semi-implicit scheme and the resulting equations were then solved using the Thomas algorithm, as outlined in Hakimzadeh (1997).

The following equations were used for the free surface boundary conditions:

$$\frac{\partial k}{\partial n} = 0 \quad (2)$$

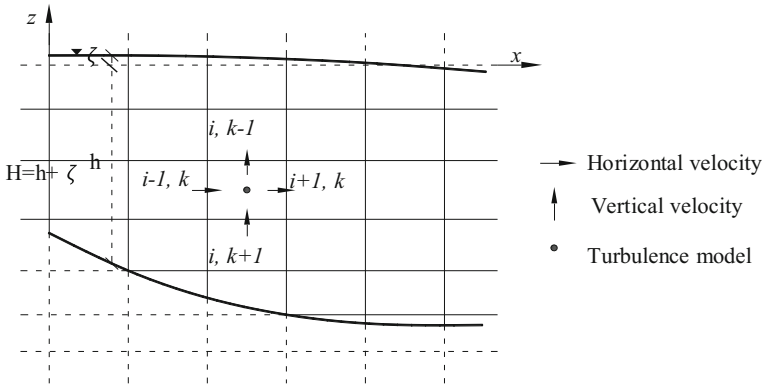


Fig. 2 Coordinate system for layer integrated equations

and for ε the following condition suggested by Krishnappan and Lau (1986) was used:

$$\varepsilon_f = \frac{c_{f\varepsilon} \left(\frac{k_f}{\sqrt{c_\mu}} \right)^{3/2}}{\kappa z_f} \tag{3}$$

where z_f = distance from the free surface to the grid centre, k_f = the corresponding value for the turbulent energy, $c_{f\varepsilon} = 0.164$, $c_\mu = 0.09$ and κ is the von Karman constant, $\kappa = 0.41$. More details of the layer integrated hydrodynamic model can be found in Faghihirad et al. (2015).

2.2.2 Sediment Transport Model

Depending upon the size and density of the bed material and the flow conditions, sediment particles can be transported in the form of bed load or suspended load. The 3-D transport equation for sediment in suspension is written as (Lin and Falconer 1996):

$$\frac{\partial S}{\partial t} + \frac{\partial}{\partial x}(uS) + \frac{\partial}{\partial y}(vS) + \frac{\partial}{\partial z}[(w-W_s)S] - \frac{\partial}{\partial x} \left(\varepsilon_x \frac{\partial S}{\partial x} \right) - \frac{\partial}{\partial y} \left(\varepsilon_y \frac{\partial S}{\partial y} \right) - \frac{\partial}{\partial z} \left(\varepsilon_z \frac{\partial S}{\partial z} \right) = 0 \tag{4}$$

where S = sediment concentration (volumetric, -), u, v, w = components of velocity in the x, y, z direction (m/s), respectively, W_s = particle settling velocity (m/s), $\varepsilon_x, \varepsilon_y$ and ε_z = sediment mixing coefficient in the x, y, z directions (m^2/s), respectively. For suspended sand particles in the range of 100-1000 μm , the following equation was used to determine W_s (van Rijn 1984):

$$W_s = 10 \frac{\nu}{D_s} \left\{ \left[1 + \frac{0.01(s-1)gD_s^3}{\nu^2} \right]^{0.5} - 1 \right\} \tag{5}$$

where ν = kinematic viscosity for clear water (m^2/s), s = specific density of suspended sediment, and D_s = representative particle diameter of the suspended sediment particles (m).

The mixing coefficients were related to the turbulent eddy viscosity through the following equations:

$$\varepsilon_x = \frac{\varepsilon_h}{\sigma_h}, \varepsilon_y = \frac{\varepsilon_h}{\sigma_h}, \text{ and } \varepsilon_z = \frac{\nu_{lv}}{\sigma_v} \tag{6}$$

where $\sigma_h, \sigma_v =$ Schmidt number in the horizontal and vertical directions respectively, with values ranging from 0.5 to 1.0, $\nu_{lv} =$ vertical eddy viscosity in a layer.

In solving Eq. (4), four type of boundaries (inflow, outflow, free surface and sediment bed boundary) need to be specified, with more details being given in Lin and Falconer (1997).

When sediment particles move within the fluid and along the bed boundary, in the form of suspended or bed load, bed level changes will generally occur. The depth-integrated mass balance equation due to sediment transport can be derived by applying the mass conservation law to a control volume in the water body from the bed to the water surface to give:

$$\frac{\partial z_b}{\partial t} + \frac{1}{1-p} \left\{ \frac{\partial}{\partial t} (H\bar{s}) + \frac{\partial}{\partial x} (q_{s,x} + q_{b,x}) + \frac{\partial}{\partial y} (q_{s,y} + q_{b,y}) \right\} = 0 \tag{7}$$

where $z_b =$ bed level (m), $p =$ porosity of the sediment material, and $q_{s,x} + q_{b,x}$ and $q_{s,y} + q_{b,y} =$ total sediment load per unit width in the x and y directions (m^2/s), respectively. The storage term $\frac{\partial}{\partial t} (H\bar{s})$ in equation (5) can be neglected, if a quasi-steady flow condition is assumed, to give:

$$\frac{\partial z_b}{\partial t} + \frac{1}{1-p} \left\{ \frac{\partial}{\partial x} (q_{s,x} + q_{b,x}) + \frac{\partial}{\partial y} (q_{s,y} + q_{b,y}) \right\} = 0 \tag{8}$$

The bed level change can be defined in terms of the mean water level (h) using the following geometrical relationship:

$$h' = h + z_b \tag{9}$$

$$\frac{\partial z_b}{\partial t} = \frac{\partial (h' - h)}{\partial t} = \frac{\partial h'}{\partial t} - \frac{\partial h}{\partial t} \text{ and } \frac{\partial h'}{\partial t} = 0 \tag{10}$$

which leads to:

$$-\frac{\partial h}{\partial t} + \frac{1}{1-p} \left(\frac{\partial}{\partial x} (q_{s,x} + q_{b,x}) + \frac{\partial}{\partial y} (q_{s,y} + q_{b,y}) \right) = 0 \tag{11}$$

In solving equation (9), an explicit finite difference scheme has been deployed. Since the hydrodynamic and sediment transport equations are solved in such a manner that each time step is divided into two half time steps, the scheme for computing bed level changes follows the general scheme. For the first half time step the discretised equation of mass balance (Eq. (9)) in the x-direction ($\Delta x = \Delta y$) is written as follows:

$$-\frac{\partial h}{\partial t} = \frac{-(lh)_{i+\frac{1}{2},j,k_{\max}}^{n+\frac{1}{2}} + (lh)_{i+\frac{1}{2},j,k_{\max}}^n - \sum_{k=1}^{k=k_{\max}-1} (lh)_{i+\frac{1}{2},j,k}^{n+\frac{1}{2}} + \sum_{k=1}^{k=k_{\max}-1} (lh)_{i+\frac{1}{2},j,k}^n}{0.5 \times \Delta t} \tag{12}$$

$$\frac{1}{1-p} \left(\frac{\partial}{\partial x} (q_{s,x} + q_{b,x}) \right) = \frac{1}{1-p} \frac{\partial q_{t,x}}{\partial x} = \frac{1}{(1-p) \times \Delta x} \left[\sum_{k=1}^{k=k_{\max}} u_{i+\frac{1}{2},j+\frac{1}{2},k}^n S_{i+\frac{1}{2},j+\frac{1}{2},k}^n (lh)_{i+\frac{1}{2},j+\frac{1}{2},k}^n - \sum_{k=1}^{k=k_{\max}} u_{i-\frac{1}{2},j+\frac{1}{2},k}^n S_{i-\frac{1}{2},j+\frac{1}{2},k}^n (lh)_{i-\frac{1}{2},j+\frac{1}{2},k}^n \right] \tag{13}$$

$$\frac{1}{1-p} \left(\frac{\partial}{\partial x} (q_{s,y} + q_{b,y}) \right) = \frac{1}{1-p} \frac{\partial q_{t,y}}{\partial y} = \frac{1}{(1-p) \times \Delta y} \left[\sum_{k=1}^{k=k_{\max}} v_{i+\frac{1}{2},j+\frac{1}{2},k}^n S_{i+\frac{1}{2},j+\frac{1}{2},k}^n (lh)_{i+\frac{1}{2},j+\frac{1}{2},k}^- - \sum_{k=1}^{k=k_{\max}} v_{i+\frac{1}{2},j-\frac{1}{2},k}^n S_{i+\frac{1}{2},j-\frac{1}{2},k}^n (lh)_{i+\frac{1}{2},j-\frac{1}{2},k} \right] \tag{14}$$

where lh = layer thickness and k = layer number. Similar discretised equations can be developed for the second half time step in the y -direction.

The main numerical solution procedure of the morphodynamic model is shown in the following flow chart (Fig. 3):

2.3 Model Verification

2.3.1 Test Case 1: Flow, Sediment Transport and bed Level Changes in a Trench

The trench experiment undertaken by van Rijn (1986) was used as the first case to test the model (see Fig. 4). The experiment, consisted of measuring flow velocity profiles, sediment concentration profiles and the bed level changes of a trench in a flume (length = 30 m, width = 0.5 m, depth = 0.7 m). In this test the mean velocity and water level at the upstream boundary were 0.51 m/s and 0.39 m, respectively. Sediments were supplied at a rate of 0.04 kg/sm at the upstream boundary to maintain an equilibrium condition. The equilibrium suspended sediment transport rate was $S_{s,0} = 0.03$ kg/sm and the bed load transport rate was $S_{b,0} = 0.01$ kg/sm. The characteristic diameters of the sediment material were: $D_{50} = 0.16$ mm and $D_{90} = 0.2$ mm. The bed-form height was in the range of 0.015–0.035 m and the roughness coefficient was set to $k_s = 0.025$ m. More details of the model configuration and hydraulic parameters can be found in van Rijn (1986).

In order to accurately predict the velocity and sediment concentration profiles 10 vertical layers of varying thickness were deployed. The thickness of the lowest layer was 0.02 m, with the thickness of subsequent layers increasing with depth. Comparisons between the predicted and measured velocity and sediment concentration profiles at five cross sections (profiles 1, 4, 6, 7 and 8 - see Fig. 4) are shown in Figs. 5 and 6. It can be seen that the velocity profiles are generally well predicted by the 3-D layer-integrated hydrodynamic model, with the shape of the velocity curves closely fitting the measured curves. The agreement between the measured and computed velocity profiles in the deceleration zone (profile 4) is closer than the acceleration zone (profile 7). It is noted that the measurements have been made in the center line of the flume, while the computations are based on cross section-layer integrated values.

The model predicted distributions of sediment concentration generally agreed well with the measured data in the middle of the trench (profile 6) and acceleration zone (profiles 7 and 8), where a rapid increase in the near-bed concentrations can be observed. The results indicate that setting up different layer thicknesses is useful. However, in the deceleration zone (profile 4) the model calculated concentrations are lower than the measured values, particularly near the bed. The results have shown that the technique used for the set up the layers in different sizes evaluated significantly useful.

One of the reasons for the under-prediction of sediment concentration may be due to the fact that in the present model an equilibrium near-bed concentration (see Lin and Falconer 1996) was used to specify the bed sediment boundary condition. Although this assumption has widely been used and shown to be valid from some numerical model studies with non-

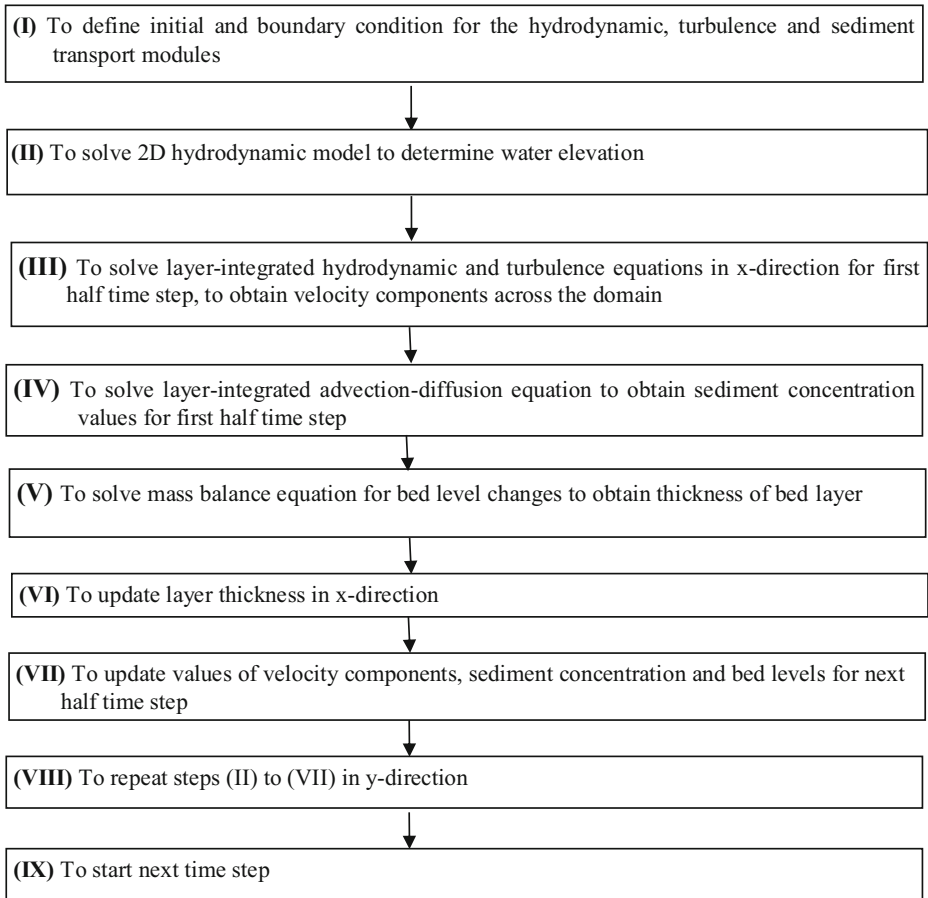


Fig. 3 Flow chart

equilibrium conditions (van Rijn 1986; Olsen and Kjellesvig 1998), it may still cause error when flow condition change rapidly at the deceleration zone in the trench

This example has also been modelled by van Rijn (1987) using a curvilinear grid model named SUTRENCH and by Kolahdoozan and Falconer (2003) using a 3D layer integrated model named GEO-TRIVAST. Figure 7 shows the measured data and the current model predicted bed level at the 15th hour into the experimental run, together with predictions made using the two other numerical models, i.e. SUTRENCH and GEOTRIVAST. It can be seen that there is a reasonable degree of similarity between the four sets of data. A different tendency at a distance of 9 m and after it is observed between SUTRENCH and others (Fig. 7). This is might be related to the scheme of mesh sizing (curvilinear grid) depends on two other numerical models.

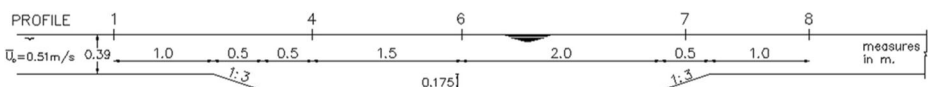


Fig. 4 Layout of trench experiment and locations of measuring profiles 1, 4, 6, 7 and 8 (taken from van Rijn 1986)

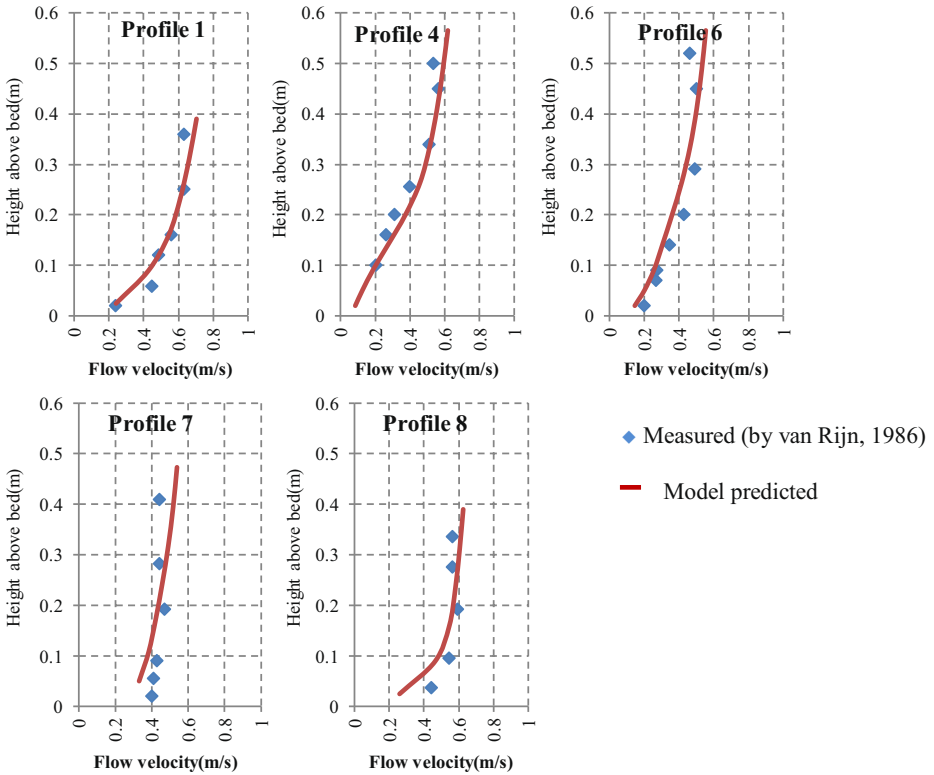


Fig. 5 Comparisons between predicted and measured velocity profiles

2.3.2 Test Case Two: Flow, Sediment Transport and Bed Level Changes in a Partially Closed Channel

To further test the model, it was then applied to predict the hydrodynamic, sediment transport and morphological processes in a 1000 m wide channel. The channel was partially closed by a dam, of length 400 m and width 100 m, as shown in Fig. 8a.

The discharge at the upstream boundary was 4000 m³/s and the water depth at the downstream boundary was 6 m. The bed material was made of sand, with $d_{50} = 200\mu\text{m}$ and $d_{90} = 300\mu\text{m}$.

This example was also tested by van Rijn (1987) and by Kolahdoozan and Falconer (2003). In the present model the grid size was set at 25 m, which was about the same size as the minimum grid size in the SUTRENCH model and equal to that used in GEO-TRIVAST. In the vertical direction the water depth was divided into 10 layers, which was the same as for the other two models.

The equilibrium suspended sediment concentration was used to specify the inlet boundary condition and a zero gradient boundary condition was set at the outlet boundary. The horizontal sediment mixing coefficients for both the x and y-directions were assumed to be constant, with values of $\epsilon_{s,x} = \epsilon_{s,y} = 0.5 \text{ m}^2/\text{s}$ and the bed roughness height was set to 0.25 m (van Rijn 1987). The bed material porosity and density were set to 0.4 and 2650 gr/m³, respectively.

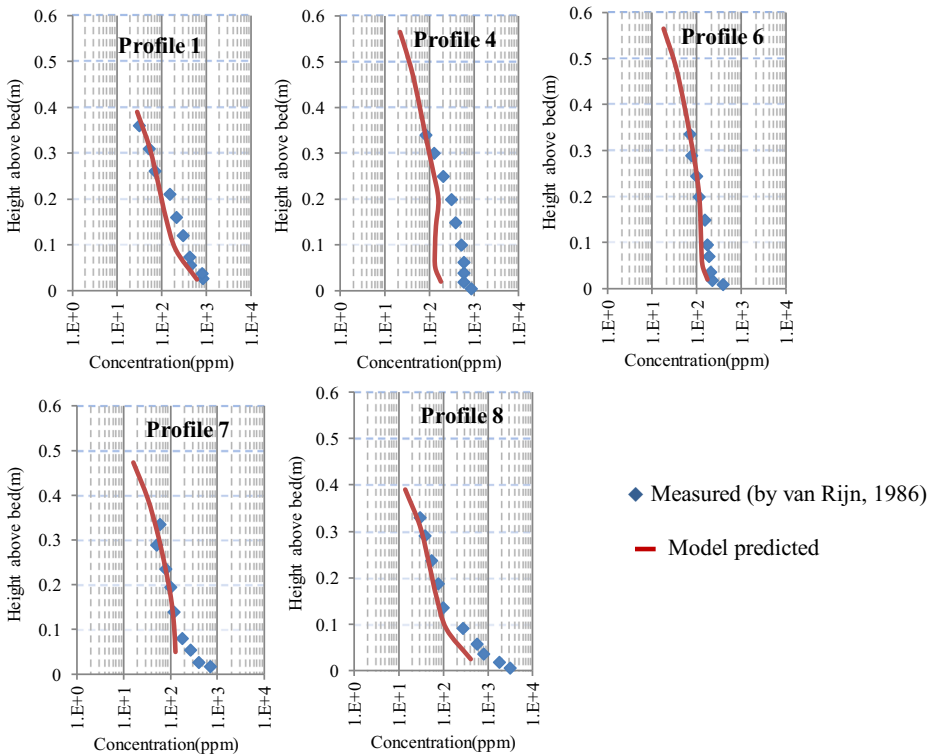


Fig. 6 Comparisons between predicted and measured sediment concentration profiles

The predictions made by the present model were compared with those obtained from the SUTRENCH and GEO-TRIVAST models. The model SUTRENCH has two versions, including a 2DV version and a quasi-3D version. For the quasi-3D model the velocity field was obtained using the depth averaged velocity components, accompanied by a logarithmic velocity profile in the vertical direction. The velocity at the inflow boundary was 0.65 m/s. The maximum velocity in the accelerating zone near the head of the headland (dam) was

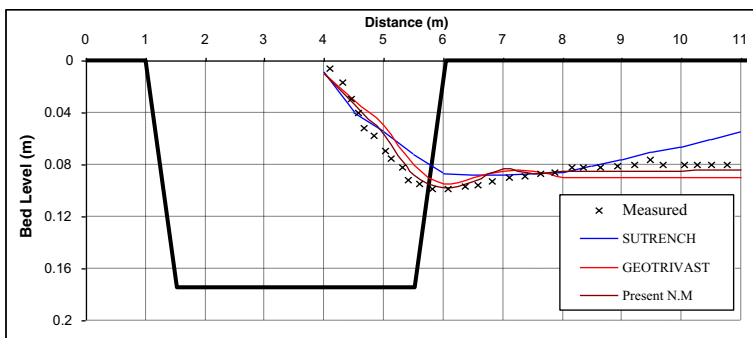
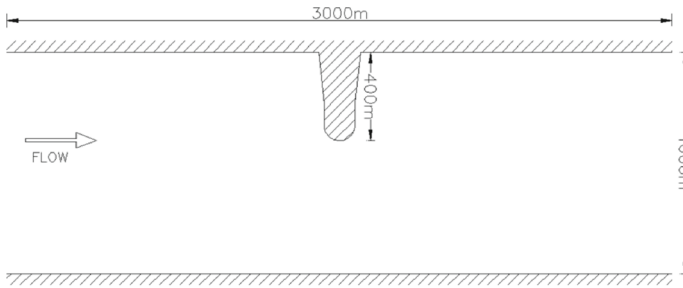
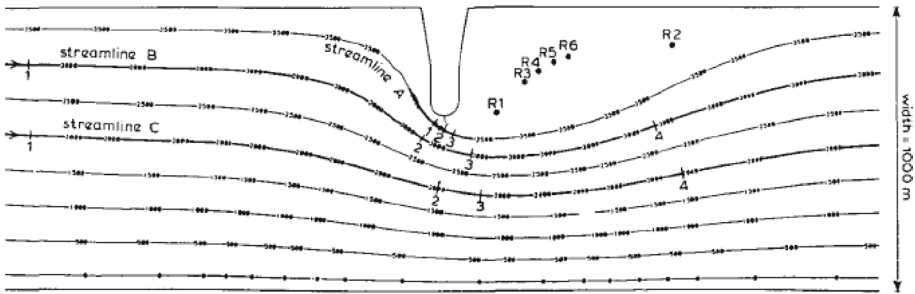


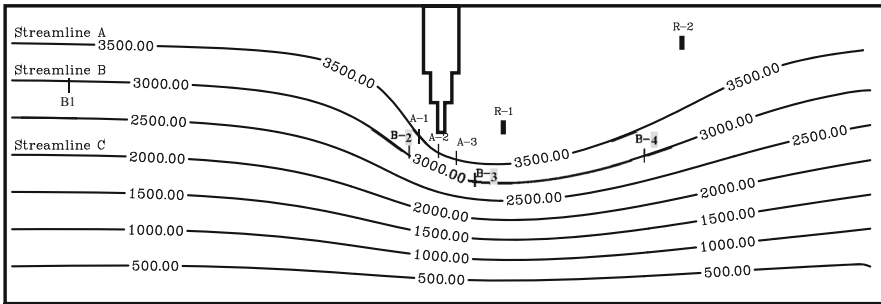
Fig. 7 Bed level profiles in the trench after 15 hours (SUTRENCH by van Rijn 1987, GEOTRIVAST by Kolahdoozan and Falconer 2003 and Present N.M = Present Numerical Model)



a) Schematic view of partially closed channel (van Rijn, 1987)



b) By SUTRENCH



c) By the presented model

Fig. 8 Streamline pattern along the channel

predicted to be 1.66 m/s using the present model. This velocity was predicted to be 1.72 m/s using the SUTRENCH model (van Rijn 1987).

Also, the streamline pattern in detail for the presented numerical model and SUTRENCH model along the channel are shown in Fig. 8b. As can be seen from Fig. 8c, a high agreement exists between both numerical results. Several nodes along the streamlines A and B, and in the recirculating zone were chosen for comparing the results of present model with those from the numerical models reported before. Due to high agreement between the streamline patterns, the locations of these nodes are physically same. Besides, this arrangement of nodes (situated in a stream line) makes a platform for presenting sediment transport results in a same stream tube of flow. Besides, the present model predicted depth averaged velocity and concentration

profiles along the streamline B and C were compared with the other models to show the accuracy and applicability of each model.

Figure 9 shows computed sediment concentration profiles along streamline B produced by the present model and the 3D model SUTRENCH. It can be seen that along streamline B the two numerical model predictions agree generally well, especially at locations away from the dam at B1 and B4. Along the water depth, the two numerical model predictions agree more closely near the bed of the channel, but near the water surface larger differences are observed, especially near the dam at B2 and B3. These differences are, however, of minor importance because most of the suspended sediment material is transported in the lower part of the water column.

Nevertheless, further research is needed to improve on the numerical schematization of the gradient type boundary conditions in the 3D model.

3 Results and Discussion

The numerical model predicted bed level changes at 6 cross-sections for case S.1 are shown in Fig. 1, together with the physical model results. As can be seen from Table 1, the simulation for S.1 was run for a much longer time in comparison with the simulation times for sites S.2 and S.3. Sediment injection continued until the same concentrations were reached at the inlet and outlet open boundaries.

From Fig. 10 it can be seen that the numerical model predicted bed level changes generally agreed well with the measured data, although there were some differences. At most locations the model predicted bed level changes were less than the measurements, but the predicted bed level change at L6-R6 was greater than the measured changes. This is thought to be due to a problem in the sediment injection system. It was found that some dry sediment injected into

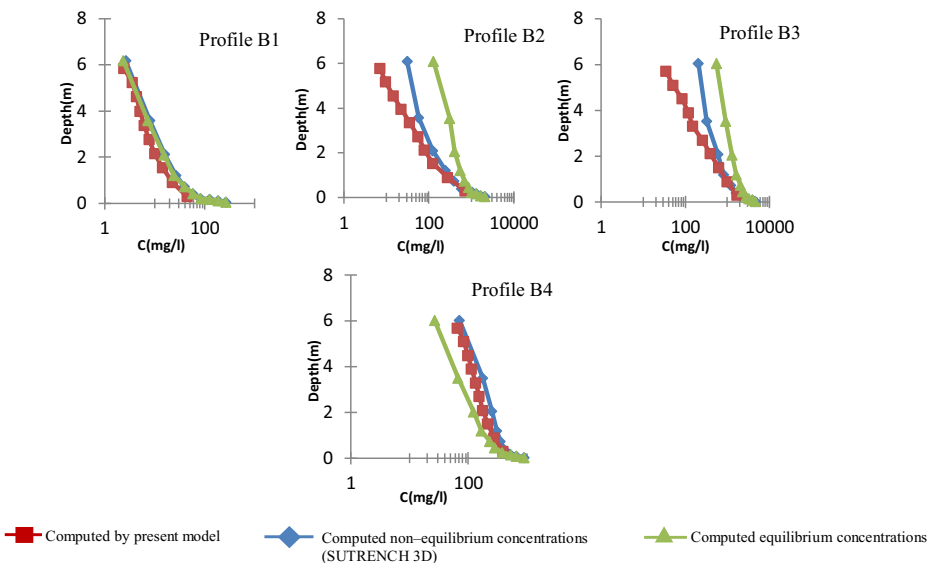


Fig. 9 Comparison between model predicted suspended sediment concentration profiles at streamline B

the reservoir from the river boundary (section L7-R7) did not initially mix well and were settled and deposited near the injection system (section L6-R6).

The bathymetries predicted by the numerical model are shown in Fig. 11. It was found that the morphodynamic model is capable of reproducing the main features observed in the physical model with an encouraging level of accuracy.

An analysis of the morphological results identifies that:

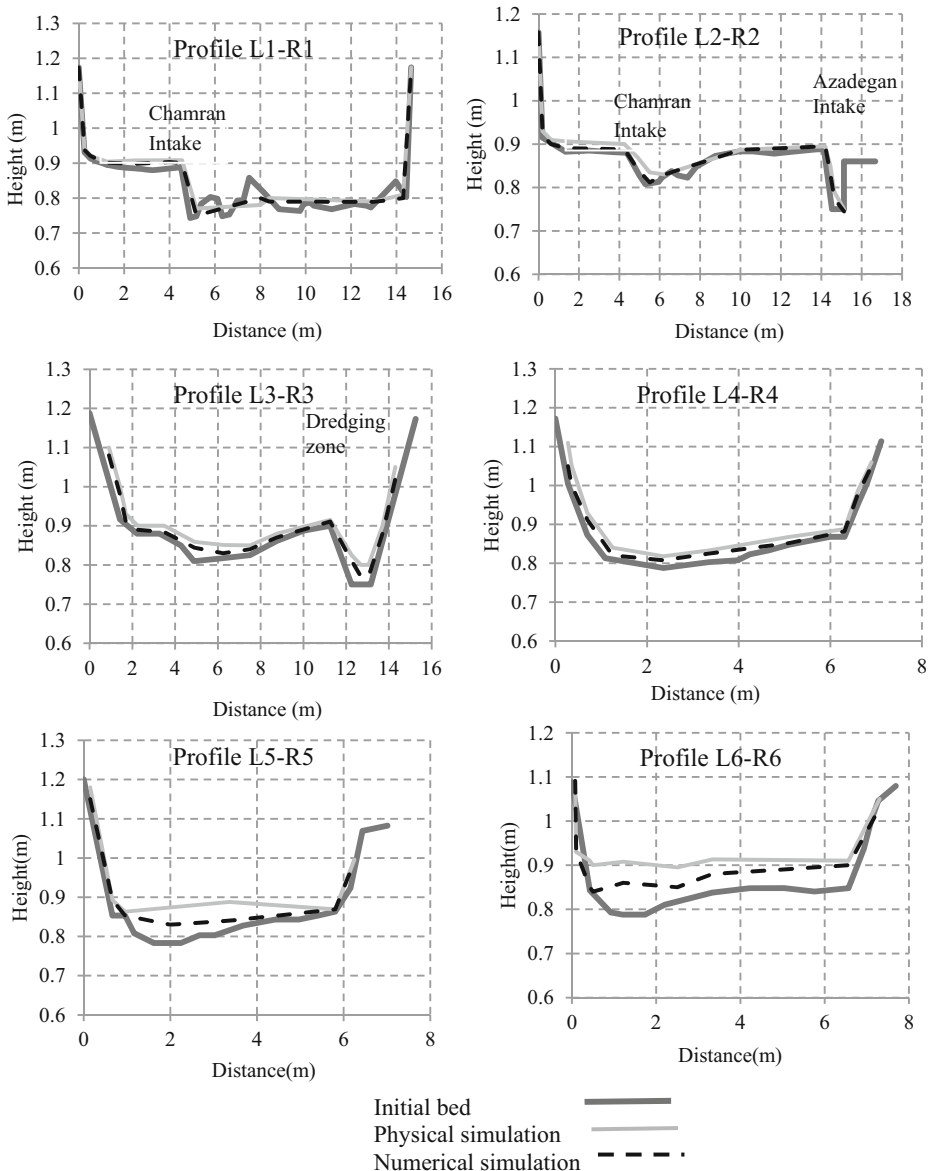


Fig. 10 Bed level changes after 48.5 hours at 6 section profiles (Scenario 1)

- (i) A deposition zone was formed in front of the Chamran intake (right corner) and the peak of this sedimentation zone then moved towards the middle region of the reservoir, resulting in a reduction in the amount of flow diverted through this intake. This phenomenon occurred for all three scenarios (i.e. S.1, S.2 and S.3), but the predicted rates of sedimentation in this zone were different for different scenarios. This bed evolution trend can be seen from Fig. 11 and profiles L1-R1, L2-R2 and L3-R3 in Fig. 1.
- (ii) When the sluice gates were open the numerical model predicted a reduction in the bed level due to erosion in front of the gates. However, the scour hole was local and did not have any noticeable effect on the sediment flushing and settling processes in front of the intakes (Fig. 11b -location A, and (c) -locations B and C).
- (iii) One dredging zone (located in front of the Azadegan intake, close to the right bank), had been identified for the purpose of delivery flow through the intake for long term water supply. The results from scenario S.3 showed that the sedimentation rate in this zone was much higher than for the other locations (Fig. 11c).
- (iv) The model predictions indicated that there was a possibility of sedimentary islands being formed upstream of the intakes, because the regulated hydraulic regime resulted in a high sediment concentration (Fig. 11c, location D).

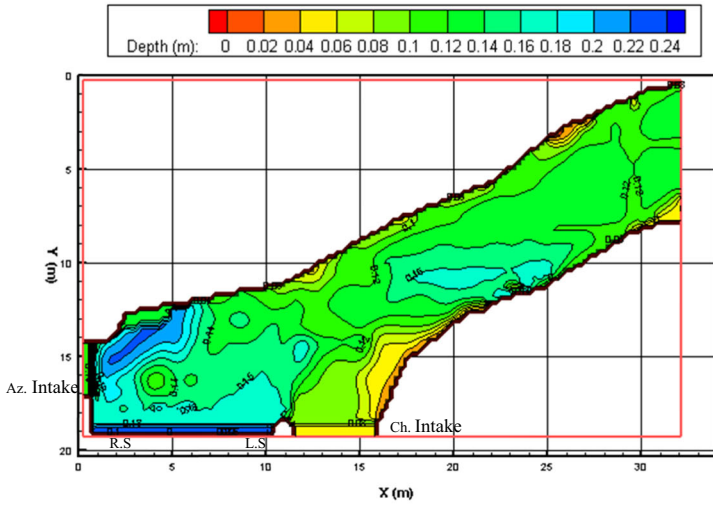
It should be pointed out that simplifications and assumptions were made in both the physical and numerical models which would have an impact on the accuracy of the model results.

4 Conclusions

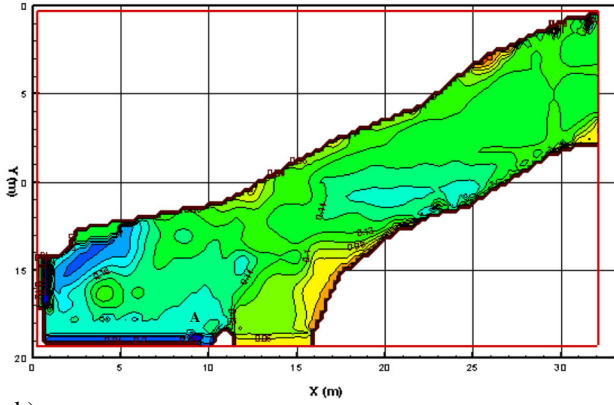
Sedimentation is a common problem that causes the capacity of reservoirs being seriously reduced; this has significant implications for reservoirs used primarily for irrigation and which is the case for the reservoir studied herein. Although many numerical model studies have been undertaken for similar types of studies, the predicted parameters from existing models generally have a high level of uncertainty. One of the main reasons for the high level of uncertainty is the lack of detailed experimental data from large scale physical model to verify the numerical model. Details are given of the refinement and application of a three-dimensional numerical morphodynamic model to predict the hydrodynamic, sediment transport and morphological processes in a river regulated reservoir, named Hamideih Reservoir. Detailed laboratory measurements of velocity and sediment distributions and bed level changes were used to validate the model. A series of scenario runs were undertaken and model predictions were compared with the measured data.

The main findings of the study are:

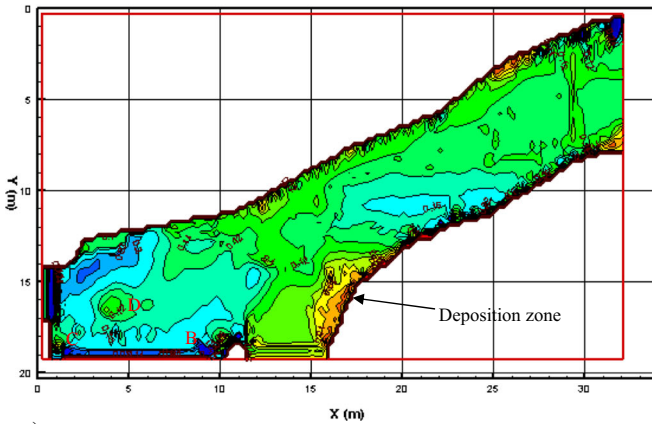
- (i) The refined model has been tested against data observed from two laboratory experiments reported in the literature. The model results compare favourably against predictions obtained using two existing numerical models.
- (ii) The 3-D layer integrated numerical model predicts morphodynamic processes in the regulated reservoir with an acceptable level of accuracy for all of the scenarios studied.



a) Initial bathymetry of Hamiddieh, physical model scale



b) Case S.2



c) Case S.3

Fig. 11 Computed bathymetry after 8 hours

- (iii) The results of this research showed that the selection of the $k-\varepsilon$ turbulence model in regulated reservoir where the Reynolds number is high but without any significant local vortex near hydraulic structures (such as gates) was the correct choice.
- (iv) An explicit method was used for discretizing the bed level change equation. This scheme is compatible with the structure of mathematical solution for hydrodynamic and sediment transport modules of the numerical model.
- (v) The location of Chamran intake has a considerable impact on the formation of the sedimentation zone in the areas adjacent to the intake.
- (vi) The operation scheme of the sluice gates does not have a considerable impact on the sediment flushing capability in the areas close to the intakes.

Acknowledgments The authors wish to thank the Water Research Institute, Iran, for providing assistance in providing the data from the physical model experiments.

Open Access This article is distributed under the terms of the Creative Commons Attribution 4.0 International License (<http://creativecommons.org/licenses/by/4.0/>), which permits unrestricted use, distribution, and reproduction in any medium, provided you give appropriate credit to the original author(s) and the source, provide a link to the Creative Commons license, and indicate if changes were made.

References

- De Vriend HJ (1985) Flow formulation in mathematical models for 2DH morphological changes. report no. R1747-5. Delft Hydraulic Laboratory, Delft
- De Vriend HJ (1986) Two- and three-dimensional mathematical modelling of coastal morphology. report no. H284-2. Delft Hydraulic Laboratory, Delft
- Faghihirad S, Lin B, Falconer RA (2010) 3D layer-integrated modelling of flow and sediment transport through a river regulated reservoir. *Int Conf Fluvial Hydraul, IAHR, Braunschweig, Germany* 2:1573–1580
- Faghihirad S, Lin B, Falconer, R.A (2015) Application of a 3D layer integrated numerical model of flow and sediment transport processes to a reservoir, *Water*, 7 (10) 5239–5257 ISSN 2073–4441, [10.3390/w7105239](https://doi.org/10.3390/w7105239)
- Falconer RA, George GD, Hall P (1991) Three-dimensional numerical modelling of wind-driven circulation in a shallow homogeneous Lake. *J Hydrol, Elsevier Sci Publ* 124:59–79
- Fischer HB, List EG, Koh RY, Imberger J, Brooks NH (1979) *Mixing and dispersion in inland and coastal waters*. Academic Press, Inc., California
- Gessler D, Hall B, Spasojevic M, Holly F, Pourtaheri H, Rappelt N (1999) Application of 3D mobile bed, hydrodynamic model. *J Hydraul Eng* 125(7):737–749
- Hakimzadeh H (1997) Turbulence modelling of tidal currents in rectangular harbours. Ph.D. thesis, Univ. of Bradford, Bradford, U.K
- Hakimzadeh H, Falconer RA (2007) Layer integrated modelling of three-dimensional recirculating flows in model tidal basins. *J Water, Port, Coast Ocean Eng, ASCE* 133(5):324–333
- Hall P (1987) Numerical modelling of wind induced lake circulation. Ph.D. Thesis, University of Birmingham, 292 pp
- Khan NM, Babel MS, Tingsanchali T (2012) Reservoir optimization-simulation with a sediment evacuation model to minimize irrigation deficits. *Water Resour Manag* 26:3173–3193
- Kocyyigit O, Lin B, Falconer RA (2005) Modelling sediment transport using a lightweight bed material. *Proc Instit Civil Eng, Maritime Eng* 158(1):3–14
- Kolahdozan M (1999) Numerical modelling of geomorphological processes in estuarine waters. Ph.D Thesis, University of Bradford, Bradford, UK, pp. 288
- Kolahdozan M, Falconer RA (2003) Three-dimensional geo-morphological modeling of estuarine waters. *Int J Sediment Res* 18(1):1–16
- Krishnappan BG, Lau YL (1986) Turbulence modelling of flood plain flows. *J Hydraul Eng* 112(4):251–266
- Lin B, Falconer RA (1996) Numerical modelling of three dimensional suspended sediment for estuarine and coastal waters. *J Hydraul Res* 34(4):435–456
- Lin B, Falconer RA (1997) Three-dimensional layer integrated modelling of estuarine flows with flooding and drying. *Estuar Coast Shelf Sci* 44(6):737–751

- Martinez RG, Saavedra IC, Power BFD, Valera E, Villoria C (1999) A two-dimensional computational model to simulate suspended sediment transport and bed changes. *J Hydraul Res* 37(3):327–344
- Nezu I, Nakagawa A (1993) Turbulence in open channel flows. IAHR Monograph Series, Balkema
- Olsen NRB (1999) Two-dimensional numerical modelling of reservoir flushing processes. *IAHR J Hydraul Res* 37(1):3–16
- Olsen NRB (2003) Three-dimensional CFD modelling of free-forming meander channel. *J Hydraul Eng* 129(5): 366–372
- Olsen NRB, Kjellesvig HM (1998) Three-dimensional numerical modelling of bed changes in a sand trap. *IAHR J Hydraul Res* 37(2):189–197
- Pu JH, Shao S, Huang Y, Hussain K (2013) Evaluations of SWEs and SPH numerical modelling techniques for dam break flows. *Eng Appl Comput Fluid Mech* 7(4):544–563
- Rodi W (2010) Large eddy simulation of river flows. *Proc Int Conf Fluvial Hydraul IAHR, Braunschweig, Germany* 1:23–32
- Rüther N, Olsen NRB (2003) CFD modelling of alluvial channel instabilities. *Proc 3rd IAHR Symposium on River, Coastal and Estuarine Morphodynamics. IAHR, Barcelona, Spain*
- Rüther N, Olsen NRB (2005a) Advances in 3D modelling of free forming meander formation from initially straight alluvial channels. *31st IAHR Congress, Seoul, South Korea*
- Rüther N, Olsen NRB (2005a) Three dimensional modelling of sediment transport in a narrow 90° channel bend. *J Hydraul Eng* 131(10):917–920
- Stephan U, Hengel M (2010) Physical and numerical modelling of sediment transport in river Salzach. *Proc Int Conf Fluvial Hydraul IAHR, Braunschweig, Germany* 2:1259–1265
- van Rijn LC (1984) Sediment transport, part II: suspended load transport. *J Hydraul Eng* 110(11):1613–1641
- van Rijn LC (1986) Mathematical modelling of suspended sediment in non-uniform flows. *J Hydraul Eng* 112(6):433–455
- van Rijn LC (1987) Mathematical modelling of morphological processes in the case of suspended sediment transport. Delft Technical University, Delft
- Wan X, Wang G, Peng Y, Bao W (2010) Similarity-based optimal operation of water and sediment in a sediment-laden reservoir. *Water Resour Manag* 24:4381–4402